Title

Single and repeated ketamine treatment induces perfusion changes in sensory and limbic networks in major depressive disorder

Authors

Sahib, Ashish K
Loureiro, Joana RA
Vasavada, Megha M
et al.

Publication Date

2020-04-01

DOI

10.1016/j.euroneuro.2020.01.017

Peer reviewed

HHS Public Access

Author manuscript

Eur Neuropsychopharmacol. Author manuscript; available in PMC 2022 February 24.

Published in final edited form as:

Eur Neuropsychopharmacol. 2020 April ; 33: 89–100. doi:10.1016/j.euroneuro.2020.01.017.

Single and repeated ketamine treatment induces perfusion changes in sensory and limbic networks in major depressive disorder

Ashish K. Sahib[a], **Joana R. Loureiro**[a], **Megha Vasavada**[a], **Antoni Kubicki**[a], **Shantanu Joshi**[a], **Kai Wang**[c], **Roger P. Woods**[a], **Eliza Congdon**[b], **Danny J.J. Wang**[c], **Michael Boucher**[b], **Randall Espinoza**[b], **Katherine L. Narr**[a,b]

[a]Ahamason-Lovelace Brain Mapping Center, Department of Neurology, University of California Los Angeles, Los Angeles, CA, USA

[b]Department of Psychiatry and Biobehavioral Sciences, University of California Los Angeles, Los Angeles, CA, USA

[c]Laboratory of FMRI Technology (LOFT), Stevens Neuroimaging and Informatics Institute, University of Southern California, Los Angeles, CA, USA

Abstract

Ketamine infusion therapy can produce fast-acting antidepressant effects in patients with major depressive disorder (MDD). Yet, how single and repeated ketamine treatment induces brain systems-level neuroplasticity underlying symptom improvement is unknown. Advanced multiband imaging (MB) pseudo-continuous arterial spin labeling (pCASL) perfusion MRI data was acquired from patients with treatment resistant depression (TRD) (N=22, mean age=35.2±9.95 SD, 27% female) at baseline, and 24 hours after receiving single, and four subanesthetic (0.5 mg/kg) intravenous ketamine infusions. Changes in global and regional CBF were compared across time points, and relationships with overall mood, anhedonia and apathy were examined. Comparisons between patients at baseline and controls (N=18, mean age=36.11±14.5 SD, 57% female) established normalization of treatment effects. Results showed increased regional CBF in the

Corresponding author: Name: Katherine L. Narr, Mailing address: 635 Charles E Young Drive South Suite 225, Los Angeles, CA 90095-7334, Phone: (310) 267-5119, narr@ucla.edu.

Contributors

The corresponding author takes responsibility for the integrity of the data and the accuracy of the data analysis. AKS analyzed the data and wrote the manuscript. JRL, MV and AK performed experiments and edited the manuscript. SJ, RPW and EC interpreted the data, KW and D.J.JW analyzed the data and interpreted it, MB performed experiments, RE and KLN designed the study and edited the manuscript. All authors contributed to and have approved the final manuscript.

ClinicalTrials.gov: Biomarkers of Fast Acting Therapies in Major Depression, https://clinicaltrials.gov/ct2/show/NCT02165449, NCT02165449

Ethical Standards

The authors assert that all procedures contributing to this work comply with the ethical standards of the relevant national and institutional committees on human experimentation and with the Helsinki Declaration of 1975, as revised in 2008.

Conflict of Interest

Authors have no disclosures or any competing financial interests in relation to the work described

cingulate and primary and higher-order visual association regions after first ketamine treatment. Baseline CBF in the fusiform, and acute changes in CBF in visual areas were related to symptom improvement after single and repeated ketamine treatment, respectively. In contrast, after serial infusion therapy, decreases in regional CBF were observed in the bilateral hippocampus and right insula with ketamine treatment. Findings demonstrate that neurophysiological changes occurring with single and repeated ketamine treatment follow both a regional and temporal pattern including sensory and limbic regions. Initial changes are observed in the posterior cingulate and precuneus and primary and higher-order visual areas, which relate to clinical responses. However, repeated exposure to ketamine, though not relating to clinical outcome, appears to engage deeper limbic structures and insula.

Keywords

Ketamine; MDD; CBF; MB pCASL; insula; fusiform

1. Introduction

Neuroimaging research continues to provide important insights into the pathophysiology of major depressive disorder (MDD) (Drysdale et al., 2017; Dunlop and Mayberg, 2014), and the physiological basis of antidepressant response (Leaver et al., 2019; Wei et al., 2018). However, despite prior research, the brain systems-level mechanisms associated with successful treatment are poorly understood (Dean and Keshavan, 2017; Duman et al., 2016). Since response to standard antidepressants is modest and protracted, and one-third of patients defined as having treatment resistant depression (TRD) are expected to fail ≥ 2 treatment trials (Gaynes et al., 2009; Nemeroff, 2007), knowledge of rapid response mechanisms is pivotal for advancing more effective interventions. Ketamine, an antagonist of N-methyl-D-aspartate (NMDA) receptors, has long been used as an anesthetic. At subanesthetic doses, ketamine is now also well-replicated to produce acute and robust antidepressant effects (Murrough et al., 2013; Zarate et al., 2013). Ketamine, a racemic mixture of equal amounts of two enantiomers, S and R ketamine, has consequently received growing off-label clinical use. Esketamine, the S(+) enantiomer, has received recent US Food and Drug Administration (FDA) approval for TRD treatment. Still, the downstream antidepressant effects of ketamine on functional neurocircuitry remain uncertain. Currently only a handful of neuroimaging studies have addressed how low-dose ketamine modulates brain function in relation to antidepressant response (Abdallah et al., 2017; Evans et al., 2018; Reed et al., 2018). Most of these studies have explored treatment effects using blood-oxygen-level-dependent (BOLD) functional magnetic resonance imaging (fMRI). Though results suggest both discrete and network-related changes in brain activity, relationships with symptom improvement are unclear, while studies addressing the neural effects of repeated ketamine therapy are lacking.

Arterial spin labelling (ASL) perfusion MRI provides a quantitative measure of regional cerebral blood flow (rCBF) and presents a complementary non-invasive functional imaging approach to BOLD fMRI. As such, perfusion MRI, demonstrated as sensitive for detecting effects of clinically effective doses of marketed drugs (Khalili-Mahani et al., 2015; Wang et

al., 2011), may offer novel understanding of the brain systems-level antidepressant effects of ketamine. A distinct advantage of ASL for longitudinal studies, is that perfusion values are reproducible over days to weeks (Chen et al., 2011; Jain et al., 2012) and directly comparable across time. This contrasts with BOLD fMRI, where only relative phasic changes secondary to neural activity can be estimated (De Simoni et al., 2013; Steward et al., 2005). ASL CBF measurements have been validated using ^{15}O-water positron emission tomography (PET) (Feng et al., 2004; Ye et al., 2000). Since perfusion is normally coupled with metabolism, ASL CBF also provides comparable information as fluorodeoxyglucose (FDG)-PET without radiation exposure (Cha et al., 2013). Several prior studies have used perfusion MRI to examine cross-sectional differences in brain function in MDD and controls. Here, rCBF differences have been identified in multiple brain regions in MDD, particularly in medial prefrontal cortex, despite clinical heterogeneity across studied samples (Chen et al., 2016; Vasic et al., 2015). However, prior studies have been compromised by low spatial resolution ASL sequences more susceptible to partial volume effects for gray (GM) and white matter (WM) CBF quantification. Pseudo-continuous ASL (pCASL) (Li et al., 2015) combined with advances in multiband echo planar imaging (MB-EPI) address several of the limitations of standard whole brain perfusion imaging. MB-EPI pCASL provides greater spatial resolution without blurring due to the long readout of 3D acquisitions. The fast imaging speed further allows acquisition of perfusion signals at multiple post-labeling delays (PLDs) to produce improved CBF estimates for detecting changes in brain function (Li et al., 2015; Shao et al., 2018).

Leveraging advanced MB pCASL imaging, in the current investigation we compared global and rCBF measured at rest in TRD patients at baseline and 24 hours after receiving single, and four serial infusions of subanesthetic ketamine, and examined relationships with clinical outcome. To our knowledge, there are currently no ASL-based studies examining the effects of either single or repeated ketamine treatment in MDD, and thus ours constitutes as a novel contribution to the field. To establish whether treatment-related changes normalize towards control values, we also compared global and rCBF between controls and TRD patients at baseline. As potentially relevant to the current investigation, increased regional cerebral glucose metabolism has been observed in MDD following a single low-dose ketamine in primary and secondary visual areas and heteromodal association cortex (occipital, postcentral, and inferior parietal cortex). Decreased metabolism is simultaneously observed in insular cortex, and in subcortical regions including the amygdala and habenula (Carlson et al., 2013). We thus hypothesized that ketamine infusion would associate with increased rCBF in sensory and association cortices, and decreased rCBF in subcortical limbic regions, and that changes associate with therapeutic responses.

2. Experimental Procedures

2.1 Subjects

Participants included 18 healthy controls (HC) and 22 DSM–5 defined (SCID, (First MB WJ, 2015)) individuals with MDD, who met criteria for TRD (i.e., failed ≥ 2 adequate antidepressant trials and had been continuously depressed for ≥ 6 months, all 20 – 64 years of age). Subjects were recruited from the Los Angeles area through advertisements, clinician

referral or clinicaltrials.gov (NCT02165449). All TRD subjects received a series of four ketamine treatments and were followed prospectively during treatment. Imaging and clinical assessments occurred at three timepoints: 1) initial baseline (TP1) occurring within one week of the first treatment; 2) 24 hours after the first ketamine infusion (TP2) and; 24 to 72 hours after the last ketamine infusion (TP3) (Figure 1A). HCs were assessed at a single time point. Demographic and clinical information is provided in Table 1.

Exclusion criteria for all participants included any unstable medical or neurological condition, current substance abuse or dependence (ascertained by laboratory testing) or substance abuse history within the preceding 3-months, current or past history of psychosis, schizophrenia, mental retardation or other developmental disorder, diagnosis of dementia and contraindication to scanning (e.g., metal implants or claustrophobia). HCs were also screened to exclude depression and/or use of any psychotropic drugs. At baseline, patients had moderate to severe depressive symptoms as per the Hamilton Depression Rating Scale (HDRS), 17–item (Hamilton, 1960) (baseline HDRS => 17). Subjects were also screened to ensure no prior psychotic reactions to medications, alcohol or illicit substances in the past, and for other physical or clinical contraindications to ketamine. All subjects provided written informed consent following procedures approved by the University of California, Los Angeles (UCLA) Institutional Review Board (IRB).

2.2 Ketamine Treatment

Patients receiving ketamine were permitted to remain on approved monoaminergic antidepressant therapy (if unchanged in the preceding 6-weeks) for the duration of the study. Benzodiazepines were discontinued the night before and morning of all study visits (e.g. scans or ketamine treatments). Patients received infusions 2–3 times a week for a total of 4 infusions. At each session, performed as an outpatient procedure, a single sub-anesthetic dose (0.5 mg/kg) of ketamine diluted in 60cc normal saline was delivered intravenously via pump over a 40-minute period in a private room at the UCLA Clinical Translational Research Center or the Resnick Neuropsychiatric Hospital. Vital sign monitoring included blood pressure, pulse oximetry, and respiratory rate recording every 3 minutes and a continuous cardiac rhythm strip. Mental status monitoring occurred during ketamine infusion and dissociative side effects were recorded 1 hr. after each infusion with the Clinician Administered Dissociative States Scale (CADSS) (Castle et al., 2017).

2.3 Clinical Measures

The HDRS (Hamilton, 1960), administered at each scanning time point, was used as the primary measure of antidepressant response. Since symptoms of apathy can be aggravated with standard antidepressant treatment (Barnhart et al., 2004), and ketamine is shown to target anhedonia specifically (Lally et al., 2015), participants also completed the Apathy Evaluation Scale (AES) (Marin et al., 1991), and the Snaith-Hamilton Pleasure Scale (SHAPS) (Snaith et al., 1995).

2.4 MRI Data Acquisition

Imaging data was acquired on a Siemens 3T Prisma MRI system at UCLA's Brain Mapping with a 32-channel head coil. Acquisition sequences were identical to those used

by the Human Connectome Project (HCP) Lifespan studies for Aging and Development (https://www.humanconnectome.org) (Harms et al., 2018). Structural scans consisted of a T1-weighed (T1w) multi-echo MPRAGE (voxel size (VS)=0.8mm isotropic; repetition time (TR)=2500ms; echo time (TE)=1.81:1.79:7.18ms; inversion time (TI)=1000ms; flip angle (34)=8.0°; acquisition time (TA)=8:22min) and a T2-weighted (T2w) acquisition (VS=0.8mm isotropic; TR=3200ms; TE=564ms; TA=6:35min), both with real-time motion correction (Tisdall et al., 2012). MB-EPI pCASL data (MB acceleration factor = 6, 60 slices with an isotropic resolution of 2.5 mm, TR/TE= 3.58/19 ms, labelling duration = 1500 ms, 5min 29 sec duration) as described in (Harms et al., 2018) was acquired to quantify CBF changes. For pCASL calibration, two additional M0 scans were collected using a proton density scan with the same readout as MB-EPI pCASL acquisition. To allow for steady state magnetization the second M0 image was used for CBF quantification. To perform distortion correction, two additional spin echo images with opposite phase encoding directions were acquired.

2.5 MRI Data Analysis

All image processing and analysis (Figure 1B) was carried out using the FMRIB software library (FSL 6.0.1) (Smith et al., 2004) and the Connectome Workbench tool (https://www.humanconnectome.org/software/connectome-workbench, version 1.3.2). FSL's topup tool corrected for MB-EPI pCASL distortions using the spin-echo images. After distortion correction, the Oxford_asl tool (Groves et al., 2009) computed calibrated CBF (ml/100g/min) maps. This procedure included motion correction, spatial regularization, 'White paper' mode that uses the kinetic model based on the ASL consensus paper (Alsop et al., 2015), voxel-wise calibration using the M0 image, partial volume correction (Chappell et al., 2011) and registration to Montreal Neurological template (2 x 2 x 2 mm^3) using the T1w anatomical scan. The calibrated CBF maps were converted into CIFTI (combined cortical surface and subcortical volume coordinate system) file format using the workbench tool using the HCP minimal preprocessing pipeline (Glasser et al., 2013). All calibrated CBF maps were visually inspected for failed registration due to motion or susceptibility artifacts. Prior to statistical analysis the calibrated CBF maps in volume as well as in CIFTI format were smoothed with a 5 mm full-width at half-maximum (FWHM) isotropic kernel. Global CBF was calculated by taking the sum of averaged GM and WM calibrated CBF. ASL data was rejected if subjects moved greater than 2.5mm or failed normalization. In total, data from 16 subjects/sessions (28 % of the sample) were excluded. Excluded data is not reported in the overall sample size including N=22 TRD patients and N=18 HCs.

2.6 Statistical Analysis

Regional effects of ketamine were confirmed with permutation testing (n=5000) using paired t-tests of calibrated CBF maps for time points examined pairwise (TP1 and TP2, TP2 and TP3, TP1 and TP3). Cross-sectional analysis between HC and TRD at baseline were performed with independent samples t-tests (age and gender as covariates) to determine effects of normalization with treatment. For volume data, tests were performed using the randomize tool (Winkler et al., 2014). Statistical thresholds were set at threshold-free cluster estimates (TFCE) $p<0.05$ (Smith and Nichols, 2009). Similar statistical tests were repeated for the surface-based CIFTI data using FSLs PALM (Winkler et al., 2014). rCBF values

from regions-of-interest (ROIs) that showed significant CBF changes in whole brain analysis were used to evaluate relationships with clinical outcome measures. Specifically, masks were created for brain regions showing significant whole brain effects with overlapping anatomical labels derived from the Freesurfer (Desikan-Killiany) atlas (Desikan et al., 2006). Mean rCBF values were extracted from these masks and correlated with clinical measures (controlling for baseline global CBF) using IBM Statistical Packages for the Social Sciences (SPSS v25). Post-hoc ROI analysis also examined the relationship between variations in baseline (TP1) rCBF with percent change (TP1-TP2) in clinical scores, as well as percent change in rCBF after single infusion (TP1-TP2) with percent change in clinical scores after serial ketamine (TP1-TP3/TP1) to determine if early effects of ketamine predict treatment response. A p-value of < 0.05 was used to establish statistical significance in these post-hoc analyses.

3. Results

3.1 Demographic and clinical results

Age and sex did not significantly differ between HC and MDD. Depression significantly improved with treatment (Table 2). Maximum improvement in mood scores was observed after serial ketamine infusion (TP3). Of the 22 TRD patients, 13 (59%) showed > 50% improvement in mood scores after serial infusion, and 7 (32%) achieved remission (HDRS<7), while only 3 patients (14%) achieved remission after the first infusion.

3.2 Cross-sectional effects between HC and TRD at baseline

At $p<0.05$ FWE correction, no differences in CBF appeared at the whole-brain voxel level between HC and TRD patients at baseline. However, HC showed significantly higher global CBF as compared to TRD ($p<.05$, Supplementary Figure 1). Consequently, follow up ROI analyses included global CBF as a covariate.

3.3 CBF changes after Ketamine Treatment

Global CBF ($p = 0.7$) did not significantly change following single or serial ketamine treatment in patients (Supplementary Figure 1). However, there was a mean increase in global CBF after the first infusion that decreased/normalized after the fourth infusion. There were no observed registration confounds for conversion of CBF maps to CIFTI format after quality control removal of data with motion artifacts (Supplementary Figure 1).

The paired t-test comparing baseline (TP1) and first ketamine infusion (TP2) revealed post-treatment increases in rCBF in parallel analysis of both CIFTI (optimized for the cortex) and volume (optimized for subcortical regions) data (Figure 2). Amongst widespread mean increases in CBF (shown in red at $p<0.01$ uncorrected, Figure 2A), significant increases (shown in yellow at $p<0.05$ FWE (family wise error) corrected, Figure 2A) were observed in the mid and posterior cingulate and proximal association areas encompassing the paracentral lobule, cuneus, precuneus, and other higher-order visual association regions including the fusiform. Results were reproduced in volume analysis at the same statistical threshold (Figure 2B). However, though trending leftward, overall the cluster was more bi-hemispheric in comparison to the surface-based CIFTI data that amplified only the left hemisphere

cluster at the statistical threshold. As shown at the uncorrected threshold of $p<0.01$ (in red), regions extend to both hemispheres in both surface and subcortical volume maps.

Clusters showing a significant increase in CBF were used to create ROIs (Figure 3) in which average CBF was correlated with mood variables. Though significant correlations were not observed between TP1-TP2 deltas, there was a significant negative relationship between baseline (TP1) CBF in the fusiform and %HDRS change (TP1-TP2) after the first infusion (Figure 4A). In addition, %CBF change (TP1-TP2) in the cuneus showed a significant positive correlation with serial %change (TP1-TP3) for overall mood (HDRS), anhedonia (SHAPS) and apathy (AES) (Figure 4B).

Compatible with our a priori hypotheses generated from PET-FDG findings (Carlson et al., 2013), a significant decrease in rCBF was observed for the paired t-test comparing TP1 and TP3 in the bilateral hippocampus and right insula (Figure 5, $p<0.01$, uncorrected), although clusters did not survive TFCE FWE thresholds. No significant differences were observed in rCBF after dichotomizing responders and non-responders after serial infusion.

4. Discussion

Motivated by the growing use of subanesthetic ketamine therapy for the short-term treatment of depressive symptoms and suicidality (Duman, 2018), this investigation applied non-invasive perfusion MRI methods to address the neurophysiological systems-level mechanisms underlying ketamine's rapid antidepressant effects. To the best of our knowledge, this is the first MRI-based perfusion study to investigate the fast-acting effects of ketamine in TRD, and to leverage advanced MB-EPI pCASL with improved spatial and temporal resolution (Li et al., 2015). Regional changes in resting-state CBF were measured 24 hours after both single and serial ketamine treatment allowing for quantitative examination of calibrated CBF in relation to ketamine response over time. Results revealed that ketamine infusion induces a robust decrease in depressive symptoms, and a significant increase of rCBF after initial infusion in brain regions encompassing the posterior and mid cingulate, precuneus, cuneus and visual association areas. In contrast, repeated treatments associated with decreased rCBF in the bilateral hippocampus and right insula, in line with prior PET findings (Carlson et al., 2013). Further, we show baseline and acute changes in rCBF in the fusiform and cuneus predict clinical response after the first infusion and following repeated treatment, respectively, suggesting that the engagement of primary and higher-order visual regions play a role in modulating rapid antidepressant response. Overall, these findings support that repeated low-dose ketamine treatment is associated with both a temporal and regional gradient of functional neuroplasticity extending from visual areas to limbic and connected insular regions (Ghaziri et al., 2018) over time and that effects relate to symptom improvement.

Prior cross-sectional studies have shown global reductions in CBF in MDD compared to controls (Baxter et al., 1985; Kanaya and Yonekawa, 1990), as well as alterations in rCBF in the sub- and supra-callosal cingulate, hippocampus, dorsolateral prefrontal cortex, inferior parietal, and occipital cortex (Duhameau et al., 2010; Vasic et al., 2015). Our results replicate previously observed reductions in global CBF in patients assessed at baseline

compared to HC, and indicate mean reductions in rCBF at the ROI level for the posterior cingulate, precuneus, cuneus, fusiform, and paracentral cortex that tend to increase in the direction of controls following single ketamine therapy [Figure 3]. At the same time, our results show significant hyper-perfusion in the right insula and bilateral hippocampus in TRD at baseline with respect to HC, that significantly decrease towards normalization over time following repeated ketamine treatment.

In this study we aimed to determine changes in CBF that occur as a consequence of neurofunctional plasticity, rather than the effects of real-time ketamine administration. During administration, low to high doses of ketamine are shown to have an immediate effect on global CBF, though these effects diminish and remain relatively static in the hours after ketamine infusion (Khalili-Mahani et al., 2015). Real-time increases in global CBF may thus reflect the timing of drug metabolism (half-life: 2–3 hours in adults). Since ketamine is mostly eliminated from the human body 24 hours post infusion, as expected, significant changes in global CBF were not shown over time in patients in this study.

After single ketamine infusion significant rCBF increases occurred in the mid and posterior cingulate, precuneus, and primary and secondary visual areas. Both the subgenual and supra-callosal cingulate play a role in integrating and regulating emotional behavior (Leech and Sharp, 2014), and are widely implicated in MDD (Hamani et al., 2011). The posterior cingulate has more extensive connections with cognitive (including internally-directed cognition) and motor-related areas (Leech and Sharp, 2014). The posterior cingulate and precuneus also form key nodes of the DMN, frequently shown to exhibit altered functional connectivity in depression (Cheng et al., 2018). Particular features of depression, such as maladaptive self-focus and rumination, and impaired attention and cognitive control, are thought to reflect DMN dysregulation (Sheline et al., 2010). Changes in perfusion in DMN network nodes may thus also contribute to the acute therapeutic effects of ketamine. Though measuring different aspects of functional plasticity, findings from resting-state fMRI studies are compatible with the current results. Specifically, a single dose of ketamine has been associated with a normalization of functional connectivity between the DMN and insula (Evans et al., 2018). Further, a prior PET-FDG investigation has reported increased glucose metabolism in the mid-cingulate cortex following single ketamine (Chen et al., 2018) in accordance with results.

Previous FDG-PET findings also report pronounced increases of glucose metabolism in bilateral occipital areas after a subanesthetic ketamine infusion in MDD (Carlson et al., 2013). These effects may reflect neuroplasticity stemming from the engagement of primary and secondary visual areas as a consequence of the dissociative and psychomimetic phenomena of ketamine. Interestingly, a recent study has shown that opioid receptor antagonism prior to intravenous ketamine administration reduces both its acute antidepressant and dissociative effects (Amiaz, 2019). Independent studies have also reported relationships between response and dissociative or psychomimetic state measured immediately after infusion (Niciu et al., 2018; Sos et al., 2013). Taken together there is considerable evidence to suggest that classical hallucinogens such as psilocybin and ketamine activate parieto-occipital regions (Vollenweider and Kometer, 2010). In our study, we observed significant relationships between acute change in rCBF in the cuneus and

subsequent antidepressant response, including change in mood and symptoms of apathy and anhedonia. It is thus possible that increased perfusion in visual areas at 24 hrs. post-treatment are linked with dissociative symptoms experienced during ketamine and could explain the association between the dissociative effects of ketamine, potentially mediated by the opiate system, and antidepressant response. Unfortunately, we were not able to address this hypothesis directly since we did not measure CBF or symptoms of dissociation with the CADSS at the actual time of infusions. Further, as consistent with recent reviews (Acevedo-Diaz et al., 2019; Short et al., 2018) CADSS scores as measured 60 minutes post treatment in our study (range: 0–5) were likely already attenuated to prohibit meaningful correlations with subsequent CBF changes. Thus, though this hypothesis is speculative, our findings nonetheless suggest that functional neuroplasticity in visual areas play a role in initial treatment response (Shaw et al., 2015).

Previous BOLD fMRI studies of intravenous ketamine in MDD have failed to report relationships between baseline or changes in functional imaging measures and clinical improvement when both are examined continuously. However, when binarizing patients into responder and non-responder groups, a recent investigation found increased global connectivity in the PFC, caudate and insula in responders only, suggesting prefrontal and striatal circuitry may be relevant to successful outcomes (Abdallah et al., 2017). Here, we observed increased perfusion in the fusiform following single ketamine, as well as a significant negative relationship between baseline rCBF and acute change in HDRS scores. Both structural (Schmaal et al., 2017) and functional abnormalities of the fusiform (Rolls et al., 2018) are demonstrated in MDD. The fusiform is involved in higher-level visual processing including in face and object recognition (Weiner and Zilles, 2016). By way of its connections with the amygdala, the fusiform also contributes to the processing of affective face stimuli, and exhibits altered patterns of brain activation in MDD (Stuhrmann et al., 2011). The fusiform may also contribute to fast acting therapeutic response. For example, ECT, also rapidly acting, is reported to enhance connectivity between amygdala and the fusiform (Wang et al., 2017). Our results thus suggest that functional plasticity of fusiform, and other visual association areas, contribute to the acute antidepressant effects of ketamine. Moreover, our results indicate that baseline rCBF in visual areas could serve as a potential biomarker of treatment response.

After serial ketamine treatment, rCBF values decreased in the bilateral hippocampus and right insula [Figure 5]. A large literature supports the hippocampus is involved in the pathophysiology of depression (Drevets et al., 2008). For example, reductions in hippocampal volume are shown to exhibit the largest effect sizes with respect to other subcortical abnormalities (Schmaal et al., 2016) in MDD, and to be linked with clinical state (Kempton et al., 2011). Recent findings also suggest other treatments for TRD, including electroconvulsive therapy (ECT), elicit changes in hippocampal rCBF that distinguish treatment responders from non-responders (Leaver et al., 2019). At the same time, the insula, which integrates cross-modal sensory and subjective state information necessary for affective processing (Chang et al., 2013), has been is implicated as contributing to specific depressive symptoms (Avery et al., 2014). Further prior research suggests right anterior insula activity changes (Brody et al., 2001) and predicts (Dunlop et al., 2015) response to standard antidepressant treatments. Connectivity changes have also been observed in the

insula following acute ketamine infusion in MDD, which might suggest a treatment-related normalization of the interaction between DMN and salience networks (Evans et al., 2018). Notably, a prior ketamine PET study showed increases in visual cortex glucose metabolism together with simultaneous decreases in insular and amygdala glucose metabolism (Carlson et al., 2013). These results are at least partially compatible with our findings showing increased rCBF in primary and secondary visual cortex after single infusion, and decreases in rCBF in deep limbic structures and the right anterior insular after repeated treatment. Taken together, our results demonstrate that neurofunctional plasticity associated with ketamine treatment changes over time in particular networks.

Several limitations should be acknowledged for the current investigation. Firstly, MB-EPI pCASL is relatively new compared to other functional imaging approaches (Wang et al., 2011), which explains the absence of clinically relevant data with which to more directly compare our data. Secondly, though we demonstrate sufficient power for detecting CBF changes over time, the limited sample size (n=22) may have led to reduced statistical power for detecting more subtle regional effects after single, or repeated ketamine treatment. However, our results show that ketamine modulates rCBF in brain regions implicated in multiple prior MDD studies, including in subcortical limbic and insula regions observed after serial ketamine at a more lenient statistical threshold. Another limitation is that ASL yields a lower SNR than fMRI, and can be more sensitive to motion. Longer scan times allowing the acquisition of a greater number of volume pairs (tag and control images) can thus ensure data is not lost due to artifacts. It should also be noted that the participants were allowed to continue concurrent stable anti-depressant medication, which may have impacted findings. Further, based on evidence suggesting possible attenuation of antidepressant effects (Andrade, 2017) and acute effects on CBF (Matthew et al., 1995), benzodiazepines were withheld prior to ketamine infusions and MRI scans. However, since only 4 patients were prescribed benzodiazepines in the current study, we were not able to examine effects in these patients separately.

CBF presents a quantitative index of brain hemodynamics related to oxygen and glucose metabolism and neurofunction. Our results show that changes in rCBF are present 24 hours after treatment demonstrating neuroplasticity occurs beyond the immediate effects of ketamine on glutamate signaling. Our findings also support that repeated low-dose ketamine therapy leads to neurofunctional plasticity in a temporally specific regional pattern. Specifically, results show neuroplasticity in primary and higher-order visual areas, as well as the posterior cingulate and precuneus following initial ketamine treatment. Further, perfusion increases at baseline and after single infusion in primary and association visual cortex may serve as a biomarker of short- and longer-term treatment response, respectively. The changes in perfusion observed in the bilateral hippocampus and right insular following serial treatment suggest that repeated exposure to ketamine may be necessary to perturb subcortical circuits, perhaps due to greater thresholds or time required for neuroplastic changes. Although our results show that racemic-ketamine induces systems-level neuroplasticity, it remains unknown if R- or S-ketamine perturb distinct neural circuitry in patients with major depression. However, each enantiomer demonstrates distinct patterns of neural response in cortical and subcortical brain regions in conscious rats (Chang et al., 2019; Masaki et al., 2019). In addition, R-ketamine exerts a longer-lasting antidepressant

effect than S-ketamine in animal models of depression and has less detrimental side-effects than *R,S*-ketamine or *S*-ketamine (Hashimoto, 2019). Further, in healthy subjects, subanesthetic administration of S- and R-ketamine each elicit regionally distinct changes in brain metabolism in association with different behavioral responses (Vollenweider et al., 1997a). Since S- and R-ketamine are associated with different patterns of metabolic activity in humans and animals (Masaki et al., 2019; Vollenweider et al., 1997b) further studies are needed on the scientific premise that warranted to establish if S- and R-ketamine enantiomers will perturb distinct neural circuits to affect functional dimensions of relevance to depression of benefit for improving clinical outcomes in depression.

Supplementary Material

Refer to Web version on PubMed Central for supplementary material.

Acknowledgemnets

This work was supported by the National Institute of Mental Health of the National Institutes of Health (Grant Nos. MH110008 [to KLN and RE], MH102743 [to KLN], and the Muriel Harris Chair in Geriatric Psychiatry (to RE)). This research was additionally supported by the UCLA Depression Grand Challenge, support for which is provided by the UCLA Office of the Chancellor and philanthropy. The content is solely the responsibility of the authors and does not necessarily represent the official views of the National Institutes of Health.

References

Abdallah CG, Averill LA, Collins KA, Geha P, Schwartz J, Averill C, DeWilde KE, Wong E, Anticevic A, Tang CY, Iosifescu DV, Charney DS, Murrough JW, 2017. Ketamine Treatment and Global Brain Connectivity in Major Depression. Neuropsychopharmacology 42, 1210–1219. [PubMed: 27604566]

Acevedo-Diaz EE, Cavanaugh GW, Greenstein D, Kraus C, Kadriu B, Zarate CA, Park LT, 2019. Comprehensive assessment of side effects associated with a single dose of ketamine in treatment-resistant depression. J Affect Disord

Alsop DC, Detre JA, Golay X, Gunther M, Hendrikse J, Hernandez-Garcia L, Lu H, MacIntosh BJ, Parkes LM, Smits M, van Osch MJ, Wang DJ, Wong EC, Zaharchuk G, 2015. Recommended implementation of arterial spin-labeled perfusion MRI for clinical applications: A consensus of the ISMRM perfusion study group and the European consortium for ASL in dementia. Magn Reson Med 73, 102–116. [PubMed: 24715426]

Amiaz R, 2019. Attenuation of Antidepressant Effects of Ketamine by Opioid Receptor Antagonism: Is It a Ketamine-Specific Effect? Am J Psychiatry 176, 250–251. [PubMed: 30818986]

Andrade C, 2017. Ketamine for Depression, 5: Potential Pharmacokinetic and Pharmacodynamic Drug Interactions. J Clin Psychiatry 78, e858–e861. [PubMed: 28858450]

Avery JA, Drevets WC, Moseman SE, Bodurka J, Barcalow JC, Simmons WK, 2014. Major depressive disorder is associated with abnormal interoceptive activity and functional connectivity in the insula. Biol Psychiatry 76, 258–266. [PubMed: 24387823]

Barnhart WJ, Makela EH, Latocha MJ, 2004. SSRI-induced apathy syndrome: a clinical review. J Psychiatr Pract 10, 196–199. [PubMed: 15330228]

Baxter LR Jr., Phelps ME, Mazziotta JC, Schwartz JM, Gerner RH, Selin CE, Sumida RM, 1985. Cerebral metabolic rates for glucose in mood disorders. Studies with positron emission tomography and fluorodeoxyglucose F 18. Arch Gen Psychiatry 42, 441–447. [PubMed: 3872649]

Brody AL, Saxena S, Stoessel P, Gillies LA, Fairbanks LA, Alborzian S, Phelps ME, Huang SC, Wu HM, Ho ML, Ho MK, Au SC, Maidment K, Baxter LR Jr., 2001. Regional brain metabolic changes in patients with major depression treated with either paroxetine or interpersonal therapy: preliminary findings. Arch Gen Psychiatry 58, 631–640. [PubMed: 11448368]

Carlson PJ, Diazgranados N, Nugent AC, Ibrahim L, Luckenbaugh DA, Brutsche N, Herscovitch P, Manji HK, Zarate CA Jr., Drevets WC, 2013. Neural correlates of rapid antidepressant response to ketamine in treatment-resistant unipolar depression: a preliminary positron emission tomography study. Biol Psychiatry 73, 1213–1221. [PubMed: 23540908]

Castle C, Gray A, Neehoff S, Glue P, 2017. Effect of ketamine dose on self-rated dissociation in patients with treatment refractory anxiety disorders. J Psychopharmacol 31, 1306–1311. [PubMed: 28922961]

Cha YH, Jog MA, Kim YC, Chakrapani S, Kraman SM, Wang DJ, 2013. Regional correlation between resting state FDG PET and pCASL perfusion MRI. J Cereb Blood Flow Metab 33, 1909–1914. [PubMed: 23963370]

Chang L, Zhang K, Pu Y, Qu Y, Wang SM, Xiong Z, Ren Q, Dong C, Fujita Y, Hashimoto K, 2019. Comparison of antidepressant and side effects in mice after intranasal administration of (R,S)-ketamine, (R)-ketamine, and (S)-ketamine. Pharmacol Biochem Behav 181, 53–59. [PubMed: 31034852]

Chang LJ, Yarkoni T, Khaw MW, Sanfey AG, 2013. Decoding the role of the insula in human cognition: functional parcellation and large-scale reverse inference. Cereb Cortex 23, 739–749. [PubMed: 22437053]

Chappell MA, Groves AR, MacIntosh BJ, Donahue MJ, Jezzard P, Woolrich MW, 2011. Partial volume correction of multiple inversion time arterial spin labeling MRI data. Magn Reson Med 65, 1173–1183. [PubMed: 21337417]

Chen G, Bian H, Jiang D, Cui M, Ji S, Liu M, Lang X, Zhuo C, 2016. Pseudo-continuous arterial spin labeling imaging of cerebral blood perfusion asymmetry in drug-naive patients with first-episode major depression. Biomed Rep 5, 675–680. [PubMed: 28101340]

Chen MH, Li CT, Lin WC, Hong CJ, Tu PC, Bai YM, Cheng CM, Su TP, 2018. Persistent antidepressant effect of low-dose ketamine and activation in the supplementary motor area and anterior cingulate cortex in treatment-resistant depression: A randomized control study. J Affect Disord 225, 709–714. [PubMed: 28922734]

Chen Y, Wang DJ, Detre JA, 2011. Test-retest reliability of arterial spin labeling with common labeling strategies. J Magn Reson Imaging 33, 940–949. [PubMed: 21448961]

Cheng W, Rolls ET, Qiu J, Xie X, Wei D, Huang CC, Yang AC, Tsai SJ, Li Q, Meng J, Lin CP, Xie P, Feng J, 2018. Increased functional connectivity of the posterior cingulate cortex with the lateral orbitofrontal cortex in depression. Transl Psychiatry 8, 90. [PubMed: 29691380]

De Simoni S, Schwarz AJ, O'Daly OG, Marquand AF, Brittain C, Gonzales C, Stephenson S, Williams SC, Mehta MA, 2013. Test-retest reliability of the BOLD pharmacological MRI response to ketamine in healthy volunteers. Neuroimage 64, 75–90. [PubMed: 23009959]

Dean J, Keshavan M, 2017. The neurobiology of depression: An integrated view. Asian J Psychiatr 27, 101–111. [PubMed: 28558878]

Desikan RS, Segonne F, Fischl B, Quinn BT, Dickerson BC, Blacker D, Buckner RL, Dale AM, Maguire RP, Hyman BT, Albert MS, Killiany RJ, 2006. An automated labeling system for subdividing the human cerebral cortex on MRI scans into gyral based regions of interest. Neuroimage 31, 968–980. [PubMed: 16530430]

Drevets WC, Price JL, Furey ML, 2008. Brain structural and functional abnormalities in mood disorders: implications for neurocircuitry models of depression. Brain Struct Funct 213, 93–118. [PubMed: 18704495]

Drysdale AT, Grosenick L, Downar J, Dunlop K, Mansouri F, Meng Y, Fetcho RN, Zebley B, Oathes DJ, Etkin A, Schatzberg AF, Sudheimer K, Keller J, Mayberg HS, Gunning FM, Alexopoulos GS, Fox MD, Pascual-Leone A, Voss HU, Casey BJ, Dubin MJ, Liston C, 2017. Resting-state connectivity biomarkers define neurophysiological subtypes of depression. Nat Med 23, 28–38. [PubMed: 27918562]

Duhameau B, Ferre JC, Jannin P, Gauvrit JY, Verin M, Millet B, Drapier D, 2010. Chronic and treatment-resistant depression: a study using arterial spin labeling perfusion MRI at 3Tesla. Psychiatry Res 182, 111–116. [PubMed: 20427157]

Duman RS, 2018. Ketamine and rapid-acting antidepressants: a new era in the battle against depression and suicide. F1000Res 7.

Duman RS, Aghajanian GK, Sanacora G, Krystal JH, 2016. Synaptic plasticity and depression: new insights from stress and rapid-acting antidepressants. Nat Med 22, 238–249. [PubMed: 26937618]

Dunlop BW, Kelley ME, McGrath CL, Craighead WE, Mayberg HS, 2015. Preliminary Findings Supporting Insula Metabolic Activity as a Predictor of Outcome to Psychotherapy and Medication Treatments for Depression. J Neuropsychiatry Clin Neurosci 27, 237–239. [PubMed: 26067435]

Dunlop BW, Mayberg HS, 2014. Neuroimaging-based biomarkers for treatment selection in major depressive disorder. Dialogues Clin Neurosci 16, 479–490. [PubMed: 25733953]

Evans JW, Szczepanik J, Brutsche N, Park LT, Nugent AC, Zarate CA Jr., 2018. Default Mode Connectivity in Major Depressive Disorder Measured Up to 10 Days After Ketamine Administration. Biol Psychiatry 84, 582–590. [PubMed: 29580569]

Feng CM, Narayana S, Lancaster JL, Jerabek PA, Arnow TL, Zhu F, Tan LH, Fox PT, Gao JH, 2004. CBF changes during brain activation: fMRI vs. PET. Neuroimage 22, 443–446. [PubMed: 15110037]

First MB WJ, K.R., Spitzer RL 2015. Structured Clinical Interview for DSM-5—Research Version (SCID-5 for DSM-5, Research Version; SCID-5-RV)

Gaynes BN, Warden D, Trivedi MH, Wisniewski SR, Fava M, Rush AJ, 2009. What did STAR*D teach us? Results from a large-scale, practical, clinical trial for patients with depression. Psychiatr Serv 60, 1439–1445. [PubMed: 19880458]

Ghaziri J, Tucholka A, Girard G, Boucher O, Houde JC, Descoteaux M, Obaid S, Gilbert G, Rouleau I, Nguyen DK, 2018. Subcortical structural connectivity of insular subregions. Sci Rep 8, 8596. [PubMed: 29872212]

Glasser MF, Sotiropoulos SN, Wilson JA, Coalson TS, Fischl B, Andersson JL, Xu J, Jbabdi S, Webster M, Polimeni JR, Van Essen DC, Jenkinson M, Consortium WU-MH, 2013. The minimal preprocessing pipelines for the Human Connectome Project. Neuroimage 80, 105–124. [PubMed: 23668970]

Groves AR, Chappell MA, Woolrich MW, 2009. Combined spatial and non-spatial prior for inference on MRI time-series. Neuroimage 45, 795–809. [PubMed: 19162204]

Hamani C, Mayberg H, Stone S, Laxton A, Haber S, Lozano AM, 2011. The subcallosal cingulate gyrus in the context of major depression. Biol Psychiatry 69, 301–308. [PubMed: 21145043]

Hamilton M, 1960. A rating scale for depression. J Neurol Neurosurg Psychiatry 23, 56–62. [PubMed: 14399272]

Harms MP, Somerville LH, Ances BM, Andersson J, Barch DM, Bastiani M, Bookheimer SY, Brown TB, Buckner RL, Burgess GC, Coalson TS, Chappell MA, Dapretto M, Douaud G, Fischl B, Glasser MF, Greve DN, Hodge C, Jamison KW, Jbabdi S, Kandala S, Li X, Mair RW, Mangia S, Marcus D, Mascali D, Moeller S, Nichols TE, Robinson EC, Salat DH, Smith SM, Sotiropoulos SN, Terpstra M, Thomas KM, Tisdall MD, Ugurbil K, van der Kouwe A, Woods RP, Zollei L, Van Essen DC, Yacoub E, 2018. Extending the Human Connectome Project across ages: Imaging protocols for the Lifespan Development and Aging projects. Neuroimage 183, 972–984. [PubMed: 30261308]

Hashimoto K, 2019. Rapid-acting antidepressant ketamine, its metabolites and other candidates: A historical overview and future perspective. Psychiatry Clin Neurosci 73, 613–627. [PubMed: 31215725]

Jain V, Duda J, Avants B, Giannetta M, Xie SX, Roberts T, Detre JA, Hurt H, Wehrli FW, Wang DJ, 2012. Longitudinal reproducibility and accuracy of pseudo-continuous arterial spin-labeled perfusion MR imaging in typically developing children. Radiology 263, 527–536. [PubMed: 22517961]

Kanaya T, Yonekawa M, 1990. Regional cerebral blood flow in depression. Jpn J Psychiatry Neurol 44, 571–576. [PubMed: 2074616]

Kempton MJ, Salvador Z, Munafo MR, Geddes JR, Simmons A, Frangou S, Williams SC, 2011. Structural neuroimaging studies in major depressive disorder. Meta-analysis and comparison with bipolar disorder. Arch Gen Psychiatry 68, 675–690. [PubMed: 21727252]

Khalili-Mahani N, Niesters M, van Osch MJ, Oitzl M, Veer I, de Rooij M, van Gerven J, van Buchem MA, Beckmann CF, Rombouts SA, Dahan A, 2015. Ketamine interactions with biomarkers of

stress: a randomized placebo-controlled repeated measures resting-state fMRI and PCASL pilot study in healthy men. Neuroimage 108, 396–409. [PubMed: 25554429]

Lally N, Nugent AC, Luckenbaugh DA, Niciu MJ, Roiser JP, Zarate CA Jr., 2015. Neural correlates of change in major depressive disorder anhedonia following open-label ketamine. J Psychopharmacol 29, 596–607. [PubMed: 25691504]

Leaver AM, Vasavada M, Joshi SH, Wade B, Woods RP, Espinoza R, Narr KL, 2019. Mechanisms of Antidepressant Response to Electroconvulsive Therapy Studied With Perfusion Magnetic Resonance Imaging. Biol Psychiatry 85, 466–476. [PubMed: 30424864]

Leech R, Sharp DJ, 2014. The role of the posterior cingulate cortex in cognition and disease. Brain 137, 12–32. [PubMed: 23869106]

Li X, Wang D, Auerbach EJ, Moeller S, Ugurbil K, Metzger GJ, 2015. Theoretical and experimental evaluation of multi-band EPI for high-resolution whole brain pCASL Imaging. Neuroimage 106, 170–181. [PubMed: 25462690]

Marin RS, Biedrzycki RC, Firinciogullari S, 1991. Reliability and validity of the Apathy Evaluation Scale. Psychiatry Res 38, 143–162. [PubMed: 1754629]

Masaki Y, Kashiwagi Y, Watabe H, Abe K, 2019. (R)- and (S)-ketamine induce differential fMRI responses in conscious rats. Synapse, e22126. [PubMed: 31397936]

Matthew E, Andreason P, Pettigrew K, Carson RE, Herscovitch P, Cohen R, King C, Johanson CE, Greenblatt DJ, Paul SM, 1995. Benzodiazepine receptors mediate regional blood flow changes in the living human brain. Proc Natl Acad Sci U S A 92, 2775–2779. [PubMed: 7708722]

Murrough JW, Perez AM, Pillemer S, Stern J, Parides MK, aan het Rot M, Collins KA, Mathew SJ, Charney DS, Iosifescu DV, 2013. Rapid and longer-term antidepressant effects of repeated ketamine infusions in treatment-resistant major depression. Biol Psychiatry 74, 250–256. [PubMed: 22840761]

Nemeroff CB, 2007. Prevalence and management of treatment-resistant depression. J Clin Psychiatry 68 Suppl 8, 17–25.

Niciu MJ, Shovestul BJ, Jaso BA, Farmer C, Luckenbaugh DA, Brutsche NE, Park LT, Ballard ED, Zarate CA Jr., 2018. Features of dissociation differentially predict antidepressant response to ketamine in treatment-resistant depression. J Affect Disord 232, 310–315. [PubMed: 29501990]

Reed JL, Nugent AC, Furey ML, Szczepanik JE, Evans JW, Zarate CA Jr., 2018. Ketamine normalizes brain activity during emotionally valenced attentional processing in depression. Neuroimage Clin 20, 92–101. [PubMed: 30094160]

Rolls ET, Cheng W, Gilson M, Qiu J, Hu Z, Ruan H, Li Y, Huang CC, Yang AC, Tsai SJ, Zhang X, Zhuang K, Lin CP, Deco G, Xie P, Feng J, 2018. Effective Connectivity in Depression. Biol Psychiatry Cogn Neurosci Neuroimaging 3, 187–197. [PubMed: 29529414]

Schmaal L, Hibar DP, Samann PG, Hall GB, Baune BT, Jahanshad N, Cheung JW, van Erp TGM, Bos D, Ikram MA, Vernooij MW, Niessen WJ, Tiemeier H, Hofman A, Wittfeld K, Grabe HJ, Janowitz D, Bulow R, Selonke M, Volzke H, Grotegerd D, Dannlowski U, Arolt V, Opel N, Heindel W, Kugel H, Hoehn D, Czisch M, Couvy-Duchesne B, Renteria ME, Strike LT, Wright MJ, Mills NT, de Zubicaray GI, McMahon KL, Medland SE, Martin NG, Gillespie NA, Goya-Maldonado R, Gruber O, Kramer B, Hatton SN, Lagopoulos J, Hickie IB, Frodl T, Carballedo A, Frey EM, van Velzen LS, Penninx B, van Tol MJ, van der Wee NJ, Davey CG, Harrison BJ, Mwangi B, Cao B, Soares JC, Veer IM, Walter H, Schoepf D, Zurowski B, Konrad C, Schramm E, Normann C, Schnell K, Sacchet MD, Gotlib IH, MacQueen GM, Godlewska BR, Nickson T, McIntosh AM, Papmeyer M, Whalley HC, Hall J, Sussmann JE, Li M, Walter M, Aftanas L, Brack I, Bokhan NA, Thompson PM, Veltman DJ, 2017. Cortical abnormalities in adults and adolescents with major depression based on brain scans from 20 cohorts worldwide in the ENIGMA Major Depressive Disorder Working Group. Mol Psychiatry 22, 900–909. [PubMed: 27137745]

Schmaal L, Veltman DJ, van Erp TG, Samann PG, Frodl T, Jahanshad N, Loehrer E, Tiemeier H, Hofman A, Niessen WJ, Vernooij MW, Ikram MA, Wittfeld K, Grabe HJ, Block A, Hegenscheid K, Volzke H, Hoehn D, Czisch M, Lagopoulos J, Hatton SN, Hickie IB, Goya-Maldonado R, Kramer B, Gruber O, Couvy-Duchesne B, Renteria ME, Strike LT, Mills NT, de Zubicaray GI, McMahon KL, Medland SE, Martin NG, Gillespie NA, Wright MJ, Hall GB, MacQueen GM, Frey EM, Carballedo A, van Velzen LS, van Tol MJ, van der Wee NJ, Veer IM, Walter H, Schnell K, Schramm E, Normann C, Schoepf D, Konrad C, Zurowski B, Nickson T, McIntosh

AM, Papmeyer M, Whalley HC, Sussmann JE, Godlewska BR, Cowen PJ, Fischer FH, Rose M, Penninx BW, Thompson PM, Hibar DP, 2016. Subcortical brain alterations in major depressive disorder: findings from the ENIGMA Major Depressive Disorder working group. Mol Psychiatry 21, 806–812. [PubMed: 26122586]

Shao X, Wang Y, Moeller S, Wang DJJ, 2018. A constrained slice-dependent background suppression scheme for simultaneous multislice pseudo-continuous arterial spin labeling. Magn Reson Med 79, 394–400. [PubMed: 28198576]

Shaw AD, Saxena N, L, E.J., Hall JE, Singh KD, Muthukumaraswamy SD, 2015. Ketamine amplifies induced gamma frequency oscillations in the human cerebral cortex. Eur Neuropsychopharmacol 25, 1136–1146. [PubMed: 26123243]

Sheline YI, Price JL, Yan Z, Mintun MA, 2010. Resting-state functional MRI in depression unmasks increased connectivity between networks via the dorsal nexus. Proc Natl Acad Sci U S A 107, 11020–11025. [PubMed: 20534464]

Short B, Fong J, Galvez V, Shelker W, Loo CK, 2018. Side-effects associated with ketamine use in depression: a systematic review. Lancet Psychiatry 5, 65–78. [PubMed: 28757132]

Smith SM, Jenkinson M, Woolrich MW, Beckmann CF, Behrens TE, Johansen-Berg H, Bannister PR, De Luca M, Drobnjak I, Flitney DE, Niazy RK, Saunders J, Vickers J, Zhang Y, De Stefano N, Brady JM, Matthews PM, 2004. Advances in functional and structural MR image analysis and implementation as FSL. Neuroimage 23 Suppl 1, S208–219. [PubMed: 15501092]

Smith SM, Nichols TE, 2009. Threshold-free cluster enhancement: addressing problems of smoothing, threshold dependence and localisation in cluster inference. Neuroimage 44, 83–98. [PubMed: 18501637]

Snaith RP, Hamilton M, Morley S, Humayan A, Hargreaves D, Trigwell P, 1995. A scale for the assessment of hedonic tone the Snaith-Hamilton Pleasure Scale. Br J Psychiatry 167, 99–103. [PubMed: 7551619]

Sos P, Klirova M, Novak T, Kohutova B, Horacek J, Palenicek T, 2013. Relationship of ketamine's antidepressant and psychotomimetic effects in unipolar depression. Neuro Endocrinol Lett 34, 287–293. [PubMed: 23803871]

Steward CA, Marsden CA, Prior MJ, Morris PG, Shah YB, 2005. Methodological considerations in rat brain BOLD contrast pharmacological MRI. Psychopharmacology (Berl) 180, 687–704. [PubMed: 15778890]

Stuhrmann A, Suslow T, Dannlowski U, 2011. Facial emotion processing in major depression: a systematic review of neuroimaging findings. Biol Mood Anxiety Disord 1, 10. [PubMed: 22738433]

Tisdall MD, Hess AT, Reuter M, Meintjes EM, Fischl B, van der Kouwe AJ, 2012. Volumetric navigators for prospective motion correction and selective reacquisition in neuroanatomical MRI. Magn Reson Med 68, 389–399. [PubMed: 22213578]

Vasic N, Wolf ND, Gron G, Sosic-Vasic Z, Connemann BJ, Sambataro F, von Strombeck A, Lang D, Otte S, Dudek M, Wolf RC, 2015. Baseline brain perfusion and brain structure in patients with major depression: a multimodal magnetic resonance imaging study. J Psychiatry Neurosci 40, 412–421. [PubMed: 26125119]

Vollenweider FX, Kometer M, 2010. The neurobiology of psychedelic drugs: implications for the treatment of mood disorders. Nat Rev Neurosci 11, 642–651. [PubMed: 20717121]

Vollenweider FX, Leenders KL, Oye I, Hell D, Angst J, 1997a. Differential psychopathology and patterns of cerebral glucose utilisation produced by (S)- and (R)-ketamine in healthy volunteers using positron emission tomography (PET). Eur Neuropsychopharmacol 7, 25–38. [PubMed: 9088882]

Vollenweider FX, Leenders KL, Scharfetter C, Antonini A, Maguire P, Missimer J, Angst J, 1997b. Metabolic hyperfrontality and psychopathology in the ketamine model of psychosis using positron emission tomography (PET) and [18F]fluorodeoxyglucose (FDG). Eur Neuropsychopharmacol 7, 9–24. [PubMed: 9088881]

Wang DJ, Chen Y, Fernandez-Seara MA, Detre JA, 2011. Potentials and challenges for arterial spin labeling in pharmacological magnetic resonance imaging. J Pharmacol Exp Ther 337, 359–366. [PubMed: 21317356]

Wang J, Wei Q, Bai T, Zhou X, Sun H, Becker B, Tian Y, Wang K, Kendrick K, 2017. Electroconvulsive therapy selectively enhanced feedforward connectivity from fusiform face area to amygdala in major depressive disorder. Soc Cogn Affect Neurosci 12, 1983–1992. [PubMed: 28981882]

Wei W, Karim HT, Lin C, Mizuno A, Andreescu C, Karp JF, Reynolds CF 3rd, Aizenstein HJ, 2018. Trajectories in Cerebral Blood Flow Following Antidepressant Treatment in Late-Life Depression: Support for the Vascular Depression Hypothesis. J Clin Psychiatry 79.

Weiner KS, Zilles K, 2016. The anatomical and functional specialization of the fusiform gyrus. Neuropsychologia 83, 48–62. [PubMed: 26119921]

Winkler AM, Ridgway GR, Webster MA, Smith SM, Nichols TE, 2014. Permutation inference for the general linear model. Neuroimage 92, 381–397. [PubMed: 24530839]

Ye FQ, Berman KF, Ellmore T, Esposito G, van Horn JD, Yang Y, Duyn J, Smith AM, Frank JA, Weinberger DR, McLaughlin AC, 2000. H(2)(15)O PET validation of steady-state arterial spin tagging cerebral blood flow measurements in humans. Magn Reson Med 44, 450–456. [PubMed: 10975898]

Zarate CA Jr., Mathews D, Ibrahim L, Chaves JF, Marquardt C, Ukoh I, Jolkovsky L, Brutsche NE, Smith MA, Luckenbaugh DA, 2013. A randomized trial of a low-trapping nonselective N-methyl-D-aspartate channel blocker in major depression. Biol Psychiatry 74, 257–264. [PubMed: 23206319]

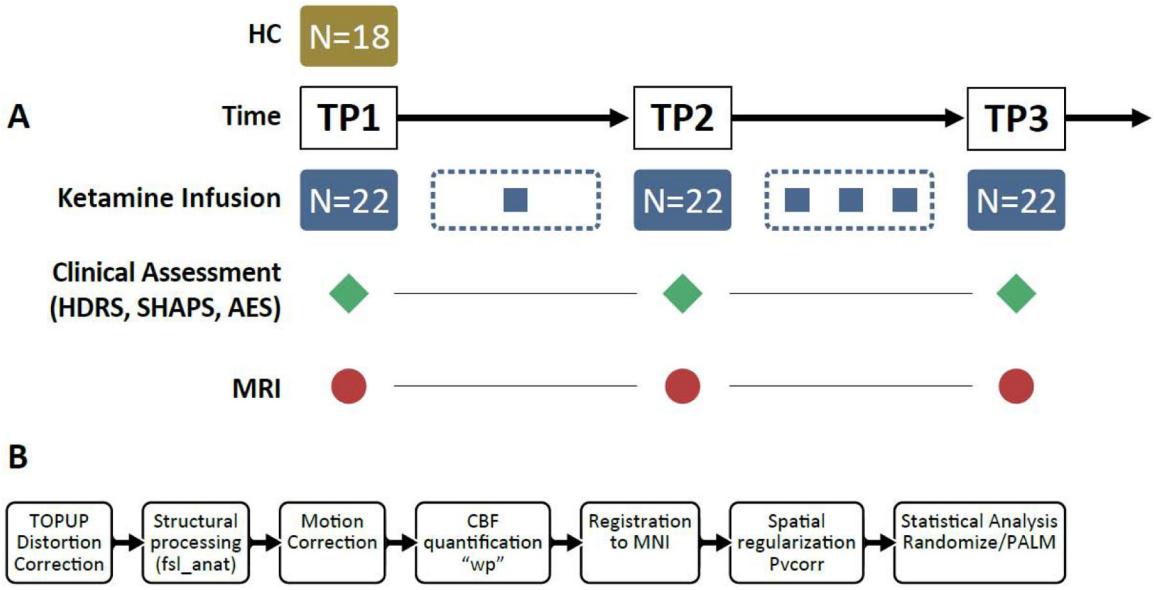

Figure 1.

A) Study design showing the timing of MRI sessions and clinical assessments; B) Imaging pre-processing pipeline where wp= white paper mode, and Pvcorr = partial volume correction.

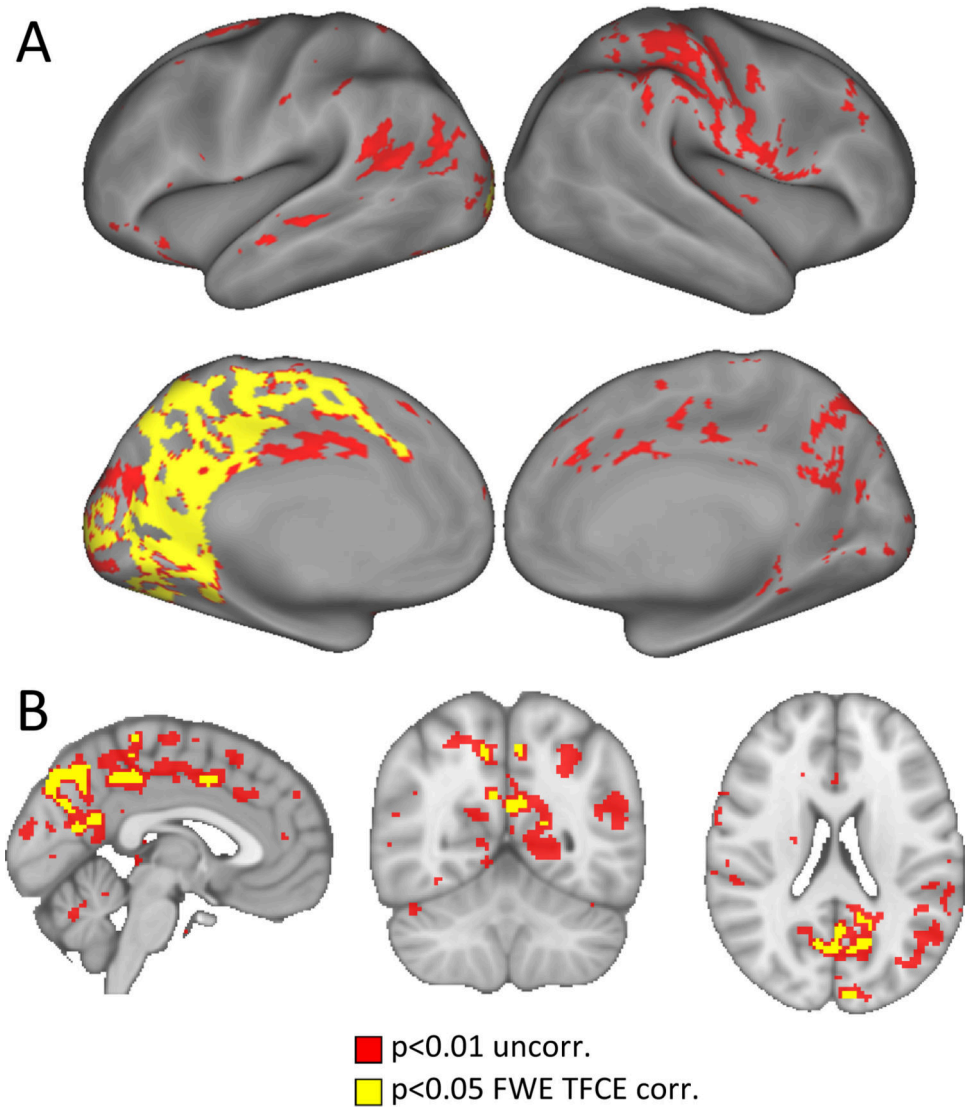

Figure 2.

A) Effect of ketamine treatment after first infusion (TP2vsTP1). Results are displayed on surface, and in B) volume space. Clusters in red correspond to p<0.01, uncorrected statistical thresholds, while clusters in yellow correspond to TFCE correction results (FWE, p<0.05).

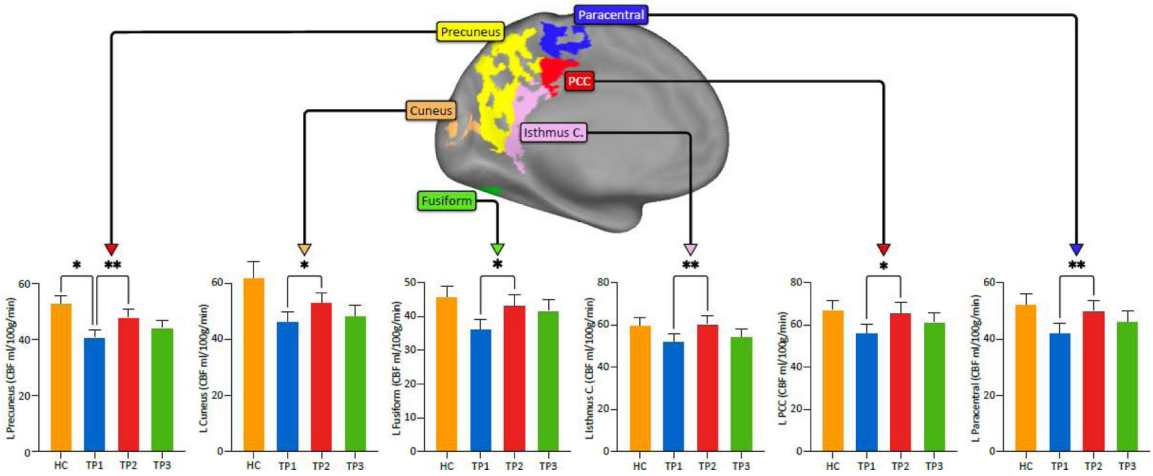

Figure 3.

Region of interests (ROIs color coded) used to perform follow-up analysis of relationships between regional CBF and mood variables. The bar plots represent the average CBF in the ROIs across ketamine treatment (*p<0.05, **p<0.01, ***p<0.001).

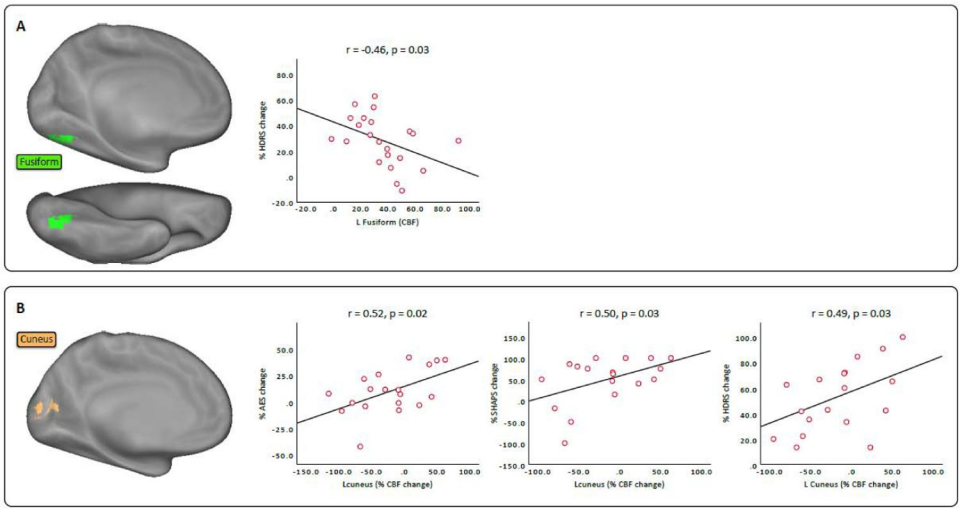

Figure 4.

Regional correlates of CBF with clinical variables. A) Baseline (TP1) CBF in the fusiform showed a significant negative relationship with acute change in HDRS (TP1-TP2); B) Acute change in CBF in the cuneus (TP1-TP2) showed a significant positive relationship with serial change (TP1-TP3) in AES, SHAPS and HDRS scores.

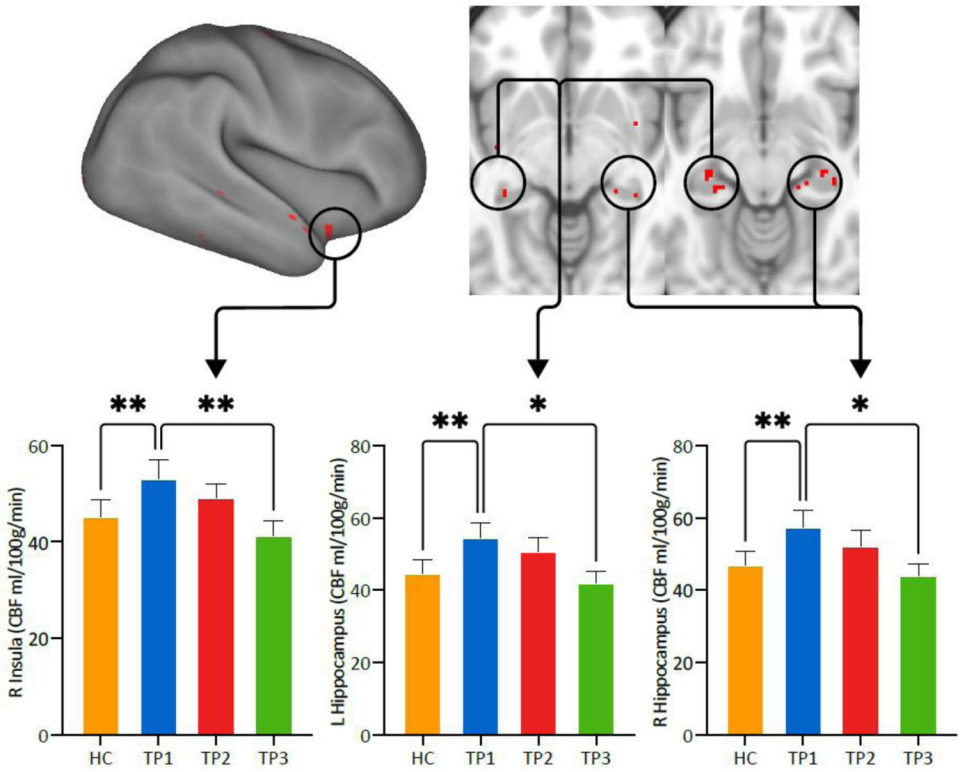

Figure 5.

CBF change after fourth infusion of ketamine (TP1vsTP3) ($p<0.01$, uncorrected). The bar plots represent the average CBF in the bilateral hippocampus and right insula across ketamine treatment (*$p<0.05$, **$p<0.01$, ***$p<0.001$).

Table 1:

Patient demographic information with mean and standard deviation (SD).

	HC Mean (SD)	MDD (TP1) Mean (SD)	MDD vs HC
Number of subjects (N)	18	22	
Gender (% female)	55.56	27.27	χ=3.31, p=0.07
Age (years)	36.11 (14.5)	35.27 (9.95)	T=0.21, p=0.83
Education (years)	9.89 (1.84)	9.72 (2.56)	T=0.22, p=0.82
Duration lifetime illness (years)	N/A	18.91 (11.91)	N/A
Current episode (years)	N/A	4.7 (5.8)	N/A

Table 2:

Clinical Measures for patients at baseline (TP1); 24 hours after the first infusion (TP2) and after fourth infusion (TP3).

	TP1	TP2	TP3	TP1vsTP2		TP2vsTP3		Tp1vsTP3	
	Mean (SD)	Mean (SD)	Mean (SD)	T	p	T	P	T	P
HDRS	19.09 (5.1)	13.68 (4.7)	8.91 (4.1)	8.67	<0.0001	5.34	0.03	10.3	<0.0001
SHAPS	8.13 (4.3)	6.77 (4.1)	3.82 (4.4)	2.4	0.22	3.58	0.04	4.75	0.008
AES	49.59 (7.6)	47.14 (7.4)	43.45 (10.6)	3.29	0.074	2.41	0.22	3.32	0.071

Abbreviations: Hamilton Depression Rating Scale (HDRS); Snaith-Hamilton Pleasure Scale (SHAPS); Apathy Evaluation Scale (AES).